

RESEARCH

Open Access



ZBTB6 promotes breast cancer progression by inhibiting ARHGAP6 transcription and modulating the STAT3 signaling pathway

Xiaojiang Tang^{1†}, Chaowei Deng^{2†}, Yang Liu¹, Shengyu Pu¹, Qi Zheng³, Yudong Zhou¹ and Na Hao^{1*} 

Abstract

Background The ZBTB (zinc finger and BTB domain-containing) protein family comprises a significant class of transcription factors that interact with various corepressors and histone/protein-modifying enzymes. This interaction facilitates chromatin remodeling and the regulation of gene silencing or activation, thereby playing a crucial role in cancer progression. However, the biological effects and molecular mechanisms of ZBTB6, a member of the ZBTB family, in cancer remain unclear.

Methods The expression levels of ZBTB6 in breast cancer (BC) were investigated through public database queries, real-time quantitative PCR (qRT-PCR), and Western blot analysis. The effects of ZBTB6 on BC cell viability were assessed via MTT assays. Flow cytometry was utilized to analyze the cell cycle distribution and apoptosis. Additionally, cell-derived xenograft experiments were conducted to study the impact of ZBTB6 on BC growth in vivo. The relationship between ZBTB6 and the ARHGAP6 promoter was evaluated via bioinformatics predictions, chromatin immunoprecipitation (ChIP) coupled with qRT-PCR, and luciferase reporter assays.

Results Our study demonstrated that ZBTB6 is highly expressed in primary BC specimens and cell lines and strongly correlated with tumor grade and poor prognosis. In vitro, ZBTB6 knockdown inhibited cell viability and cell cycle progression while promoting apoptosis; conversely, ZBTB6 overexpression elicited the opposite effects. In vivo, the inhibition of ZBTB6 expression in BC cells significantly suppressed tumor growth. Furthermore, we identified ARHGAP6 as a transcriptional target downstream of ZBTB6, with ZBTB6 binding to the promoter region of ARHGAP6 to repress its transcription. Notably, ARHGAP6 can exert an inhibitory effect on tumors by attenuating STAT3 activity. Our results indicate that ZBTB6 overexpression enhances the STAT3 signaling pathway, whereas ARHGAP6 overexpression counteracts the effects of ZBTB6 overexpression in BC cells.

Conclusion These findings suggest that ZBTB6 promotes breast cancer progression by repressing the transcription of ARHGAP6 and activating the STAT3 signaling pathway. Consequently, ZBTB6 may serve as a potential prognostic biomarker or therapeutic target for breast cancer patients.

Keywords ZBTB6, ARHGAP6, Breast cancer, Cell cycle, Apoptosis, STAT3 signaling pathway

[†]Xiaojiang Tang and Chaowei Deng contributed equally to this work.

*Correspondence:

Na Hao

1120150460@mail.nankai.edu.cn

¹Department of Breast Surgery, the First Affiliated Hospital of Xi'an Jiaotong University, Xi'an, Shaan'xi Province 710061, China

²Department of Cell Biology and Genetics, Institute of Genetics and Developmental Biology, School of Basic Medical Sciences, Xi'an Jiaotong University Health Science Center, Xi'an, Shaanxi 710061, China

³Department of Medical Oncology, Affiliated Shaanxi Provincial Cancer Hospital, College of Medicine, Xi'an Jiaotong University, Xi'an, Shaanxi 710061, China



© The Author(s) 2025. **Open Access** This article is licensed under a Creative Commons Attribution-NonCommercial-NoDerivatives 4.0 International License, which permits any non-commercial use, sharing, distribution and reproduction in any medium or format, as long as you give appropriate credit to the original author(s) and the source, provide a link to the Creative Commons licence, and indicate if you modified the licensed material. You do not have permission under this licence to share adapted material derived from this article or parts of it. The images or other third party material in this article are included in the article's Creative Commons licence, unless indicated otherwise in a credit line to the material. If material is not included in the article's Creative Commons licence and your intended use is not permitted by statutory regulation or exceeds the permitted use, you will need to obtain permission directly from the copyright holder. To view a copy of this licence, visit <http://creativecommons.org/licenses/by-nc-nd/4.0/>.

Background

Although considerable progress has been made in the screening, diagnosis and treatment of breast cancer (BC), this disease remains a major public health problem [1]. With 2.3 million new cases diagnosed in 2020, BC has become the most common type of cancer among women worldwide, accounting for 11.7% of all cancer diagnoses [2]. Although the possibilities resulting from improved early detection and treatment modalities are great, many patients remain diagnosed (or overdiagnosed) at late stages, resulting in a higher mortality risk [3]. Treatment options include surgery, chemotherapy, radiotherapy, targeted therapy and endocrine therapy [4, 5]. Nevertheless, even with an expanding array of treatment options, several patients still suffer from suboptimal restoration and long-term survival, especially those with recurrent disease [6]. Consequently, existing treatment measures are still insufficient to deliver a complete and powerful course of BC remedies. There is an unmet need for the discovery of novel biomarkers and therapeutic targets to improve long-term survival, as well as quality of life, in BC patients.

The ZBTB (zinc finger and BTB domain-containing) family of proteins constitutes a pivotal class of transcription factors characterized by unique structural features that facilitate their involvement in various biological processes. Members of this family typically contain a C-terminal zinc finger domain responsible for recognizing and binding specific DNA sequences, along with an N-terminal BTB (broad-complex, tram-track and bric-a-brac) domain that promotes protein-protein interactions, particularly in the formation of homo or heterodimers [7, 8]. In the regulation of gene transcription, ZBTB proteins function primarily as transcriptional repressors by recruiting corepressors (such as N-CoR, SMRT, and HDACs) to gene promoter regions through their BTB domains, thereby inhibiting the transcription of target genes [7]. Consequently, ZBTB proteins play diverse roles in regulating a variety of cellular processes, such as proliferation and apoptosis, significantly influencing cell growth and death by modulating the expression of cell cycle-related genes [9]. Moreover, ZBTB proteins affect the proliferation and survival of tumor cells by modulating critical pathways, including the Wnt signaling pathway, which is correlated with patient prognosis [10]. Certain members of this family, such as BCL6 and LRE, are recognized as proto-oncogenes or tumor suppressors in cancer; BCL6 promotes tumorigenesis in non-Hodgkin's lymphoma, whereas PLZF is acknowledged as a tumor suppressor in acute promyelocytic leukemia [11, 12]. Notably, ZBTB1 has been linked to DNA repair processes, highlighting its significant role in tumorigenesis [13]. Conversely, dysregulation of ZBTB24 has been associated with the development of human lymphomas,

underscoring its potential involvement in tumor suppression [14]. While the current literature primarily addresses hematological tumors, the roles of ZBTB proteins in other tumor types (such as solid tumors) are under intensive investigation. Overall, ZBTB family proteins play multifaceted roles in various cancers [7]. Dysfunction of these genes may contribute to tumorigenesis and progression, making them significant targets for the study of tumor development. ZBTB6, a member of the ZBTB family, has been reported to be potentially associated with clinical outcomes in esophageal cancers [15] and has the potential to serve as a therapeutic target for type I nasopharyngeal carcinoma [16]. However, the role of ZBTB6 in a variety of tumors, including breast cancer, has not been definitively investigated, and the biological effects of ZBTB6 in cancer and the underlying molecular mechanisms are still unclear.

ARHGAP6 (Rho GTPase-activating protein 6) is a key member of the RhoGAP family and is primarily responsible for regulating intracellular signaling by promoting GTP hydrolysis in Rho GTPases [17]. This regulatory function significantly affects cell morphology, motility, proliferation, and apoptosis [18]. In various human diseases, particularly cancer, the expression levels of ARHGAP6 exhibit considerable variability, with reduced expression correlating with tumorigenesis and disease progression. For example, decreased levels of ARHGAP6 in breast cancer have been associated with poor prognosis [18]. Diminished expression in lung adenocarcinoma is linked to increased resistance to the chemotherapeutic agent cisplatin (DDP) [19]. Additionally, in bladder and cervical cancers, ARHGAP6 exhibits tumor-suppressive properties by inhibiting cell proliferation and migration [20, 21]. Consequently, ARHGAP6 tends to play a negative role in tumorigenesis and progression.

In this study, our experimental findings demonstrated that ZBTB6 promotes cell proliferation and inhibits apoptosis by regulating the STAT3 signaling pathway in BC cells. Mechanistically, we identified ARHGAP6 as a transcriptional downstream target of ZBTB6. ARHGAP6 is an important signaling molecule. It inhibits the activation of the intermediate RhoA, which directly leads to the tyrosine phosphorylation of STAT3 and thus the activation of STAT3, and the activation of STAT3 is closely related to cell survival signaling pathways [22–24]. Notably, ZBTB6 enhances the STAT3 signaling pathway by downregulating ARHGAP6 expression. Collectively, these findings suggest that ZBTB6 drives BC progression through the ARHGAP6/STAT3 axis. This work provides new insights into the intrinsic mechanisms underlying BC development and offers a theoretical framework for considering ZBTB6 as a promising prognostic indicator or chemotherapeutic target.

Methods

Clinical specimens

A total of 61 BC patients were enrolled in this study, from which clinical tissue samples and corresponding clinicopathological characteristics, including age, sex, and initial stage, were collected. All samples were obtained from the Department of Surgical Oncology at the First Affiliated Hospital of Xi'an Jiaotong University. None of these patients received chemotherapy or radiotherapy prior to surgery, as clearly documented in their pathological records. This study was approved by the Ethics Committee of the Health Sciences Centre at Xi'an Jiaotong University, ensuring that the entire research process adhered to ethical standards.

Reagents and antibodies

Super ECL prime reagents (Cat: S6008-100 mL) were purchased from US Everbright® Inc. (Suzhou, China). RIPA lysis buffer, phenylmethanesulfonyl fluoride (PMSF) and the transfection reagent Lipofectamine™ 2000 were obtained from Thermo Fisher Scientific (New York, USA). Annexin V-APC (2005128) and propidium iodide (2048964) were obtained from Invitrogen (California, USA). 3-(4,5)-Dimethylthiazolium di-phenyltetrazolium bromide (MTT) (M5655) and dimethyl sulfoxide (DMSO) (D5879) were purchased from Sigma-Aldrich (St. Louis, MO, USA). The anti-ZBTB6 (PA5-112925) antibody was purchased from Invitrogen (California, USA). ARHGAP6 (SC-81938), STAT3 (SC-293151), p-STAT3 (sc-81523), Survivin (SC-10811), c-Myc (SC-789), Histone H3 (SC-517576) and GAPDH (SC-47724) were purchased from Santa Cruz Biotechnology (California, USA). Mouse IgG (B900620) antibodies were purchased from Proteintech Group (Wuhan, China).

Cell culture

The cell lines utilized in this study included HMECs, BT-747 cells, T-47D cells and MCF-7 cells, all of which were obtained from Procell Life Science & Technology Co. Ltd. (Shanghai, China). To ensure the reliability of our experiments, each cell line was assessed for mycoplasma contamination via Lonza's MycoAlert kit, which was provided by the supplier. The cell lines were cultured in 1640 medium supplemented with 1% penicillin-streptomycin solution and 10% fetal bovine serum under standard conditions (5% CO₂ and 37 °C).

Quantitative and reverse transcription PCR

Total RNA was extracted from the collected cells and human tissues via TRIzol reagent (Invitrogen, Carlsbad, CA, USA) following the manufacturer's instructions. The extracted total RNA was further reverse transcribed to synthesize cDNA via the PrimeScript™ RT Kit (TaKaRa

Biotechnology Co., Ltd., Dalian, China). cDNA was subsequently detected via the iCycler iQ Multicolor qRT-PCR Detection System (Bio-Rad, Hercules, CA, USA) for qRT-PCR experiments to analyze gene expression levels. The results were normalized for glyceraldehyde-3-phosphate dehydrogenase (GAPDH) gene expression, and each reaction was repeated three times to ensure the reliability and consistency of the data. All primers used were as follows:

ZBTB6-F: 5'- TGGTGTGCGAAAATGGGCAGT-3'
ZBTB6-R: 5'- AGGAACTTCAGCCACTCTGC-3'
ARHGAP6-F: 5'- TGAGGTCAGTCCCCATCC-3'
ARHGAP6-R: 5'- GCATCTTTCTGCTCGTCC-3'
GAPDH-F: 5'-GCCGTATCGCTCAGACAC-3'
GAPDH-R: 5'-GCCTAATACGACCAAATCC-3'

Transfection and infection experiments and plasmids

The short hairpin RNA (shRNA) lentiviruses used in this study to target human ZBTB6 were obtained from Gene Pharma Co. Ltd. (Shanghai, China). Small interfering RNAs (siRNAs) for the knockdown of ARHGAP6 and ZBTB6, along with their negative controls, were also obtained from the same company as follows:

Negative siRNA (NC-siRNA) sense: 5'-UUCUCCGAA CGUGUCACGUTT-3'.

Negative siRNA (NC-siRNA) antisense: 5'- ACGUGA CACGUUCGGAGAATT-3'.

ZBTB6 siRNA-1 sense: 5'- CAGAAAGAUUUGUGCA CCATT-3'.

ZBTB6 siRNA-1 antisense: 5'- UGGUGCACAAAUCU UUCUGTT-3'.

ZBTB6 siRNA-2 sense: 5'- GUUAUGGUACAGUGAG UGATT-3'.

ZBTB6 siRNA-2 antisense: 5'- UCACUCACUGUACC AUAACCTT-3'.

ARHGAP6 siRNA-1 sense: 5'- GAAACTGGATTAC TAGGATT-3'.

ARHGAP6 siRNA-1 antisense: 5'- UCCUAGUGAAUC CAGUUUCTT-3'.

ARHGAP6 siRNA-2 sense: 5'- CAUUAAAAAGCGGA UCCAATT-3'.

ARHGAP6 siRNA-2 antisense: 5'- UUGGAUCCGCU UUUUAAUGTT-3'.

sh-Control:

5'- AAAAGAGGCTTGCACAGTGCATTCAAGACG TGCCTGTGCAAGCCTCTTTT-3'.

ZBTB6 shRNA:

5'- TGGAGAACTGATGTGGATTTTCTCGAGTGG TGCACAAATCTTTCTGTTTTTTC-3'.

The recombinant plasmids containing full-length cDNAs of human ZBTB6 as well as ARHGAP6 were cloned and inserted into the PCDH-CMV-MCS-EF1-Hygro vector, which was purchased from Youbao Company (Changsha, China).

For the cell transfection experiments, BT-747 and MCF-7 cells were seeded in 6-well plates during the logarithmic growth phase, with 2×10^5 cells and 2 mL of medium added to each well, and incubated overnight at 37 °C. Transfection was subsequently optimized with siRNA and an overexpression plasmid (2 µg/well) via Lipofectamine™ 2000 (6 µL/well) for 72 h.

For the infection experiments, BT-747 cells were infected with lentivirus at 40% confluency, with each infection lasting 12 h. A total of two infections were performed. Following infection, the cells were treated with puromycin (Life Technologies, New York, USA) for 36 h to select successfully integrated cells. The surviving cells were then frozen and stored in liquid nitrogen for future experiments.

Cell viability detection

The cells were seeded in 96-well culture plates at a density of 3000 cells per well, with 100 µL of 1640 medium added to each well. The cells were subsequently treated with either small interfering RNA (siRNA) or overexpression plasmids for 24, 48, or 72 h. At the specified time points, 10 µL of a 5 mg/mL MTT solution was added to each well, followed by incubation at 37 °C for 4 h. After incubation, the suspension was removed, and 150 µL of DMSO was added to each well to dissolve the formed formazan crystals. Finally, the absorbance values at 492 nm were measured via a multifunctional microplate reader (POLARstar OPTIMA, BMG LabTechnologies, Germany) to assess cell viability.

Cell cycle analysis

The treated BC cells were cultured in six-well plates until they reached 50% confluence within 24 h prior to analysis. The cells were then collected via trypsin digestion and resuspended in phosphate-buffered saline (PBS). For fixation, the cells were treated overnight with ice-cold 70% ethanol at 4 °C. The cells were subsequently stained with 50 µg/mL propidium iodide (PI) and 50 µg/mL DNase-free RNase A for 20 min at room temperature. Finally, flow cytometry was conducted via a fluorescence-activated cell sorter (FACSCalibur, BD Biosciences, San Jose, CA, USA) to analyze the cell cycle.

Apoptosis analysis

Treated BC cells were cultured in six-well plates and allowed to reach 50% confluence within 24 h prior to analysis. The cells were harvested through trypsin digestion and subsequently resuspended in phosphate-buffered saline (PBS). Next, the cells were stained with the Annexin-V FITC Apoptosis Detection Kit according to the manufacturer's instructions. Apoptosis analysis was then conducted via flow cytometry with a FACSCalibur flow cytometer (BD Biosciences, San Jose, CA, USA) for

data acquisition. Finally, the population of apoptotic cells was analyzed and quantified via ModFit software.

Western blot analysis

This study utilized samples from BC clinical tissues, normal breast tissues, and BC cells. For protein extraction, RIPA lysis buffer supplemented with PMSF and protease inhibitors (Roche, Indianapolis, IN, USA) was used, using Nuclear Extraction Kit SK-0001 (signosisinc) for nuclear protein extraction. Equal amounts of extracted proteins were loaded onto a 10% SDS polyacrylamide gel for separation, followed by transfer to polyvinylidene difluoride (PVDF) membranes. After transfer, the membranes were blocked at room temperature for 2 h with 5% BSA. The membranes were then incubated overnight at 4 °C with the primary antibody. The membranes were subsequently incubated with secondary antibodies (peroxidase-labeled anti-mouse and anti-rabbit antibodies) for 2 h at room temperature. Finally, the membranes were treated with Super ECL reagent for signal detection, and the resulting luminescent signals were scanned, recorded, and quantified via Syngene GBox (Syngene, UK).

Subcutaneous tumor xenografts

This study adhered to the Guidelines for Animal Health and Use established by the Ministry of Science and Technology of China (2006). A total of ten five-week-old female nude mice were obtained from Huaifu Kang Biotechnology Co., Ltd. (Beijing, China) and randomly divided into two groups. The mice were housed in a specific pathogen-free (SPF) environment for one week to acclimatize to their new surroundings. Subsequently, BT-747 cells transfected with negative control shRNA or ZBTB6 shRNA (1.5×10^7 cells per mouse) were injected subcutaneously into the left upper backs of the mice in both groups via a 0.1 mL serum-free RPMI-1640 suspension. To mitigate pain, isoflurane was used for nasal anesthesia, which is known for its rapid onset and ease of control; mice typically recover within 2 min after cessation of anesthesia. If any mouse exhibited abnormal signs during anesthesia, the anesthesia equipment was immediately turned off, and emergency treatment was provided to ensure safety. Isoflurane is excreted entirely through respiration and does not affect mouse metabolism, thereby minimizing interference with the experimental results. To maintain sterility, the skin of the mice was disinfected with 75% medical alcohol before and after subcutaneous injection.

One week after injection, the tumor volume was measured every three days after injection under stringent feeding conditions, and the following formula was used: [tumor volume = (length × width²)/2]. Prior to tumor collection, the mice were anesthetized nasally to alleviate pain, after which they were euthanized, and the tumors

were harvested. The carcasses were weighed, frozen at -20 °C, and subsequently processed for photographic documentation.

Immunohistochemical staining

The paraffin-embedded tumors were initially sectioned at a thickness of 5 mm and subjected to dewaxing and hydration. The sections were then placed in citrate buffer (pH 6.0) and heated to 95 °C in a microwave oven for 20 min to facilitate antigen retrieval. Following antigen retrieval, endogenous peroxidase activity was inhibited, and nonspecific binding was prevented by blocking with normal goat serum. Subsequently, an anti-ZBTB6 antibody diluted in PBS (1:20) was applied to the paraffin sections, which were subsequently incubated overnight at 4 °C. Upon completion of the incubation, a horseradish peroxidase-conjugated secondary antibody was added, and the sections were further incubated. Afterward, the DBA reagent was introduced for color development, and the final results were observed under a microscope. Hematoxylin restaining was performed to enhance contrast.

ChIP-qRT-PCR assay

The reagents and equipment utilized included a chromatin immunoprecipitation (ChIP) kit (Millipore), Dynabeads Protein A (Thermo Fisher Scientific, USA), and a QIAquick PCR purification kit (QIAGEN, Germany). In BT-747 and MCF-7 cells, cross-linking was achieved via the addition of 1% formaldehyde for 15 min, followed by quenching with glycine. The DNA was subsequently sheared into fragments ranging from 200 to 800 base pairs via ultrasonic treatment. These DNA fragments were then incubated with ZBTB6 or IgG antibodies for 12 h at 4 °C to facilitate specific immunoprecipitation. Following the extraction of DNA-protein complexes via Dynabeads Protein A, the complexes were eluted with TE buffer at 65 °C. The next step involved inverse cross-linking of the complexes at 65 °C for 8 h. Finally, the isolated DNA products were purified via a QIAquick PCR purification kit for quantitative reverse transcription PCR (qRT-PCR) analysis. The corresponding gene-specific primers used are as follows:

ARHGAP6 (ChIP)-Primer 1-F: 5'- CTGGATGGCCTC TAAGACTCCAGCA-3'.

ARHGAP6 (ChIP)-Primer 1-R: 5'- GCCGGGAGCGC GGTGGACGCGCCCT-3'.

ARHGAP6 (ChIP)-Primer 2-F: 5'- CGCTCCCGGCGC CGCGAGAACTTCC-3'.

ARHGAP6 (ChIP)-Primer 2-R: 5'- GAGCCTCTGCAG TCGGAAGAGTGGG-3'.

ARHGAP6 (ChIP)-Primer 3-F: 5'- CAAGGGTTGTTC CAAGCTCAAGTT-3'.

ARHGAP6 (ChIP)-Primer 3-R: 5'- CACCGTGGGCAC GCAGTCTTTGGAG-3'.

ARHGAP6 (ChIP)-Primer 4-F: 5'- CCGGGACCTCCA AAGACTGCGTGCC-3'.

ARHGAP6 (ChIP)-Primer 4-R: 5'- GGGCTGCGAATA GCGTGTTCCTCTC-3'.

ARHGAP6 (ChIP)-Primer 5-F: 5'- GAGGAACACGCT ATTCGCAGCCCAG-3'.

ARHGAP6 (ChIP)-Primer 5-R: 5'- CTCTACACGTCC TGGCCGCCCTT-3'.

ARHGAP6 (ChIP)-Primer 6-F: 5'- ACGTGTAGAGCT GGAGGAATGCCGG-3'.

ARHGAP6 (ChIP)-Primer 6-R: 5'- TCCTCGCCGCTT GCAGTTTGGCGC-3'.

GAPDH (ChIP)-F: 5'-GTGGCAAAGTGGAGATTGT T-3'.

GAPDH (ChIP)-R: 5'-CTCGCTCCTGGAAGATGG-3'.

Luciferase reporter assay

The dual-luciferase expression plasmids pGL3-luc and pGL3-ARHGAP6-luc were constructed by AuGCT DNA-SYN Biotechnology (Beijing, China). Subsequently, either the pGL3-luc or pGL3-ARHGAP6-luc plasmid was transfected into BC cells to evaluate its effectiveness. Additionally, ZBTB6 siRNA was cotransfected with a negative control siRNA (NC-siRNA) into BC cells previously transfected with pGL3-ARHGAP6-luc, along with the overexpression of ZBTB6 and vector transfection. Forty-eight hours posttransfection, BC cells were harvested, and luciferase activity was quantified via the Dual-Luciferase Reporter System (Promega, USA).

Public clinical data sets analysis

Data regarding ZBTB6 and ARHGAP6 expression as well as prognosis were downloaded from The University of Alabama at Birmingham CANcer data analysis Portal (UALCAN) (<https://ualcan.path.uab.edu/index.html>). The ChIP data of ZBTB6 (CistromeDB: 65189; 65192; 65190) were downloaded from the Cistrome Data Browser (<http://cistrome.org/db/>). Data regarding the correlation between ZBTB6 and ARHGAP6 was downloaded from GEPIA 2 (<http://gepia2.cancer-pku.cn/#correlation>).

Statistical analysis

The experimental results of this study consisted of three replicates of quantitative data derived from independent experiments, with all the data presented as the means ± standard errors of the means (SEMs). Statistical analyses were conducted via SPSS 19.0 software (Abbott Laboratories, Chicago, IL), and the quantitative data are expressed as the means ± standard deviations and were analyzed according to their characteristics. The statistical methods employed included Student's t test, two-way

ANOVA, and the Pearson chi-square test. A significance threshold of $P < 0.05$ was established to determine statistically significant results.

Results

High expression of ZBTB6 in BC is related to clinicopathologic characteristics

To elucidate the role of ZBTB6 in the progression of BC, we first examined the correlation between ZBTB6 expression and the clinicopathological features of BC. Analysis through the University of Alabama at Birmingham Cancer Data Analysis Portal (UALCAN) revealed that ZBTB6 was significantly overexpressed in BC tissues compared with normal breast tissue ($P < 0.05$) and correlated with nodal metastasis and TP53 mutation status ($P < 0.05$) (Fig. 1a–c). Moreover, Kaplan–Meier survival analysis via UALCAN data indicated that high ZBTB6 expression was correlated with poor prognosis ($P < 0.01$) (Fig. 1d).

We subsequently investigated ZBTB6 expression levels in 61 BC tissues alongside matched adjacent nontumor tissues via quantitative real-time PCR (qRT-PCR), confirming the significant upregulation of ZBTB6 mRNA in BC tissues compared with normal tissues ($P < 0.05$) (Fig. 1e). Western blot analysis demonstrated that ZBTB6 expression was also elevated in BC tissues compared with normal breast tissues (Fig. 1f).

To support subsequent *in vitro* experiments, we validated these findings in BC cell lines (BT-747, T-74d, and MCF-7) via Western blotting and qRT-PCR. The results indicated that ZBTB6 expression was significantly higher in BC cell lines than in normal human breast epithelial cell lines (HMECs) (Fig. 1f, g). In summary, these findings suggest that ZBTB6 may serve as a potential biomarker for the progression of human breast cancer.

ZBTB6 promotes BC cell proliferation and inhibits apoptosis *in vitro*

Given the clinical significance of ZBTB6 in BC, we investigated the effects of ZBTB6 gain and knockdown on the malignant growth potential of BC cells to elucidate the role of ZBTB6 in this context. Using the BC cell lines BT-747 and MCF-7, which exhibit high levels of ZBTB6 expression, we performed *in vitro* experiments. qRT-PCR and Western blotting analyses demonstrated that ZBTB6 siRNAs significantly reduced ZBTB6 expression in BT-747 and MCF-7 cells (Fig. 2a, b; $P < 0.01$), whereas the ZBTB6 overexpression vector effectively increased ZBTB6 levels (Fig. 2a, b; $P < 0.01$). MTT assays revealed that ZBTB6 knockdown led to decreased viability in BC cells (Fig. 2c; $P < 0.01$), whereas ZBTB6 overexpression resulted in increased viability (Fig. 2d; $P < 0.01$). Flow cytometry analysis revealed that ZBTB6 knockdown caused cell cycle arrest in the G0/G1 phase (Fig. 2e;

$P < 0.01$) and increased the percentage of apoptotic cells (Fig. 2g; $P < 0.01$), whereas ZBTB6 overexpression had the opposite effect (Fig. 2f, h; $P < 0.01$).

ZBTB6 ShRNA inhibits BC cell proliferation and promotes apoptosis *in vitro* and *in vivo*

To assess the role of ZBTB6 in regulating BC cell growth more precisely, we generated a stable ZBTB6-knockdown BT-747 cell line via a shRNA lentivirus transfection system. qRT-PCR and Western blotting confirmed that ZBTB6 shRNAs significantly suppressed ZBTB6 expression in BT-747 cells (Fig. 3a, b; $P < 0.01$), subsequently inhibiting BC cell viability, as demonstrated by MTT assays (Fig. 3c; $P < 0.01$). Similar to the results observed with ZBTB6 siRNAs, flow cytometry revealed that ZBTB6 shRNA also induced cell cycle arrest in the G0/G1 phase (Fig. 3d; $P < 0.01$) and increased the percentage of apoptotic cells (Fig. 3e; $P < 0.01$).

Subsequently, we subcutaneously injected BT-747 cells with ZBTB6 shRNA or control shRNA into 5-week-old female nude mice. Compared with those in the control groups, the growth, volume, and weight of the tumors derived from ZBTB6 shRNA-expressing cells were significantly lower (Fig. 3f–h). qRT-PCR and immunohistochemical staining were conducted to verify the downregulation of ZBTB6 in tumors derived from ZBTB6 shRNA-transduced BT-747 cells (Fig. 3i, j; $p < 0.01$). Together, these data indicate that ZBTB6 promotes the malignancy and progression of BC cells.

ZBTB6 binds the promoter of ARHGAP6 to mediate its transcription

In light of the role of ZBTB6 as a transcription factor, we utilized bioinformatics analysis (Cistrome Data Browser) to identify potential target genes of ZBTB6, further elucidating the molecular mechanisms by which ZBTB6 regulates BC progression. Our findings indicate that ZBTB6 can bind to the promoter region of ARHGAP6 (Fig. 4a). Data from The Cancer Genome Atlas (TCGA) revealed a negative correlation between ZBTB6 and ARHGAP6 expression in human BC tissues (Fig. 4b; $P < 0.01$). Notably, qRT-PCR analysis of 61 BC tissues and their matched adjacent nontumor counterparts revealed a significant negative correlation between ZBTB6 mRNA and ARHGAP6 mRNA expression (Fig. 4c; $P < 0.01$). Importantly, we confirmed that ZBTB6 binds to the ARHGAP6 promoter in BT-747 and MCF-7 cells via a chromatin immunoprecipitation (ChIP)-quantitative PCR (QPCR) assay (Fig. 4d; $P < 0.01$). To further validate these findings, we employed a dual-luciferase reporter system in which the target sequence of the ARHGAP6 promoter was inserted into the luciferase gene of the pGL3 reporter plasmid, which was subsequently transfected into BT-747 and MCF-7 cells. Luciferase activity

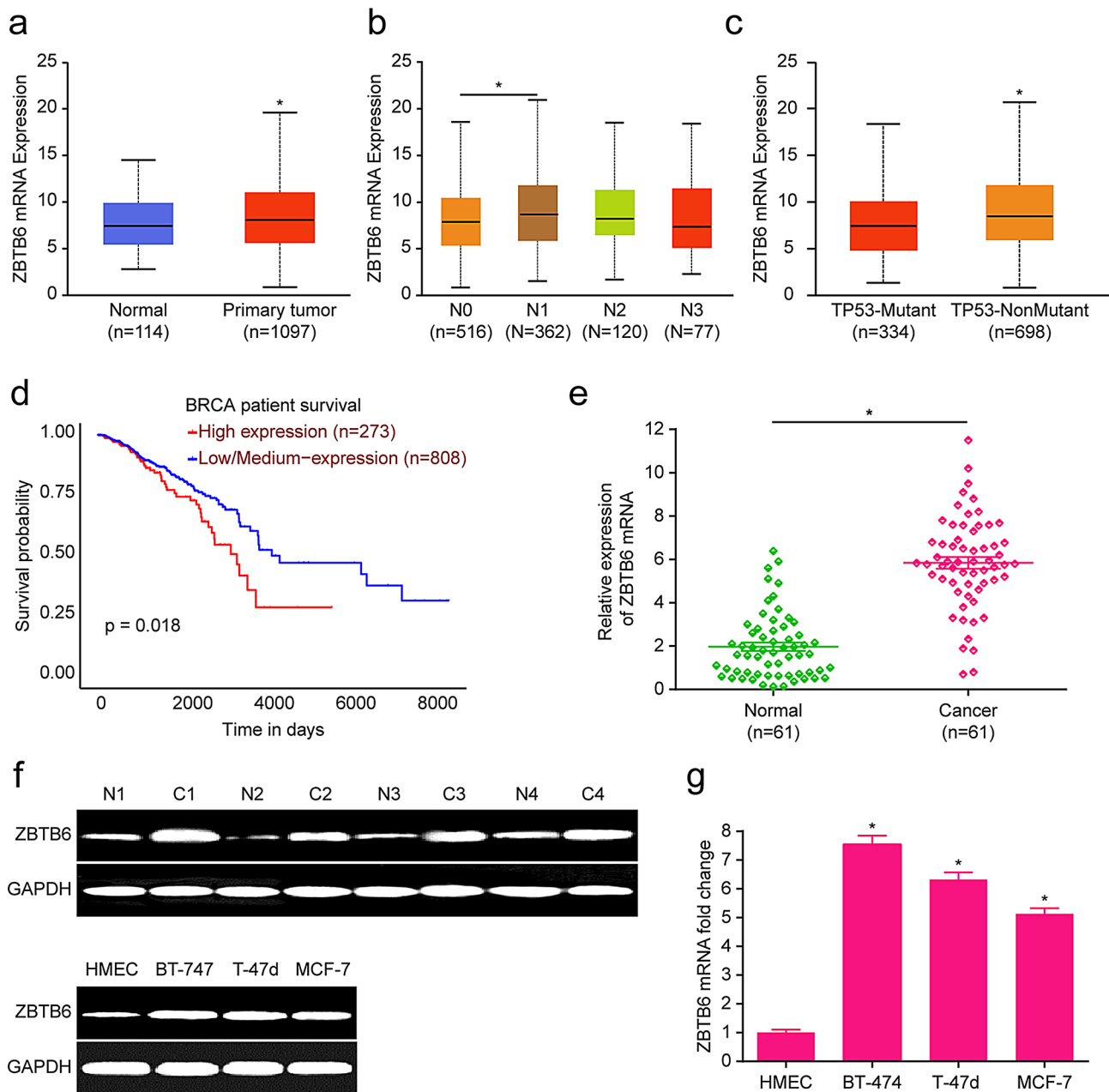


Fig. 1 High expression of ZBTB6 in BC is related to clinicopathologic characteristics. **(a)** ZBTB6 expression in BC patients. **(b)** Correlation between ZBTB6 expression and nodal metastasis in BC patients. **(c)** Correlation between ZBTB6 expression and TP53 mutation status in BC patients. **(d)** OS estimation datasets from patients in the high ZBTB6 expression correlation group compared with those in the low expression correlation group. **(e)** ZBTB6 mRNA expression in BC tissues versus normal breast tissues ($n=61$; $P<0.01$). **(f)** ZBTB6 protein expression in BC tissues and cell lines. GAPDH was used as an internal reference. **(g)** ZBTB6 mRNA expression in BC cells (BT-747, T-47d, and MCF-7) versus a normal human breast epithelial cell line (HMEC). GAPDH was used as an internal reference. Each experiment was performed in triplicate. The quantitative data in **(a-c, g)** were analyzed via Student's *t* test, and the quantitative data in **(d)** were analyzed via Pearson's chi-square test; * $p<0.05$

was measured after 48 h, revealing a significant increase in luciferase activity in the pGL3-ARHGAP6-luc group compared with the pGL3-luc group (Fig. 4e; $P<0.01$). ZBTB6 siRNAs and the ZBTB6 overexpression vector were subsequently cotransfected with pGL3-ARHGAP6-luc into BT-747 and MCF-7 cells. We observed a remarkable increase in luciferase activity in the ZBTB6 siRNA

groups compared with the negative control siRNA group (Fig. 4f; $P<0.01$), whereas luciferase activity was significantly lower in the ZBTB6 overexpression vector group than in the control vector group (Fig. 4g; $P<0.01$). To further assess the effect of ZBTB6 on ARHGAP6 expression, we performed qRT-PCR and Western blotting analyses. The results indicated that ZBTB6 siRNAs markedly

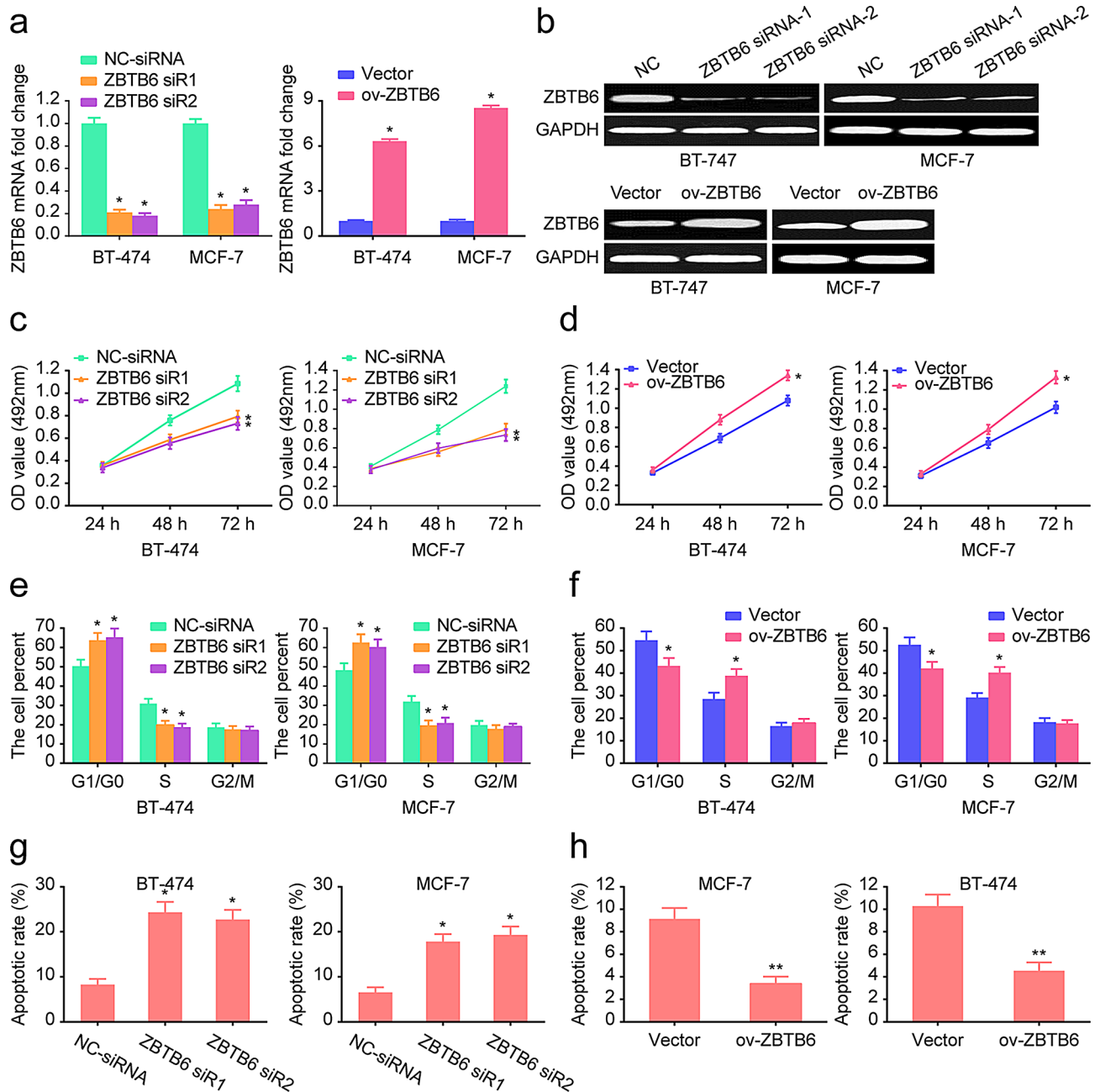


Fig. 2 ZBTB6 promotes BC cell proliferation and inhibits apoptosis in vitro. **(a)** ZBTB6 mRNA expression after transfection with ZBTB6 siRNA and ZBTB6-overexpression plasmid in BC cells. GAPDH was used as an internal reference. **(b)** ZBTB6 protein expression after transfection with ZBTB6 siRNA and ZBTB6-overexpression plasmid in BC cells. GAPDH was used as an internal reference. **(c)** Viability of BC cells after transfection with ZBTB6 siRNA. **(d)** Viability of BC cells after transfection with the ZBTB6-overexpression plasmid. **(e)** The cell cycle of BC cells after transfection with ZBTB6 siRNA was analyzed by flow cytometry. **(f)** The cell cycle distribution of BC cells after transfection with the ZBTB6-overexpression plasmid was analyzed by flow cytometry. **(g)** Apoptosis of BC cells after transfection with ZBTB6 siRNA was examined via flow cytometry. **(h)** Apoptosis of BC cells after transfection with the ZBTB6-overexpression plasmid was examined via flow cytometry. Each experiment was performed in triplicate. The quantitative data in **(c, d)** were analyzed via Pearson's chi-square test, and the quantitative data in **(a, e-h)** were analyzed via Student's t test; * $p < 0.05$

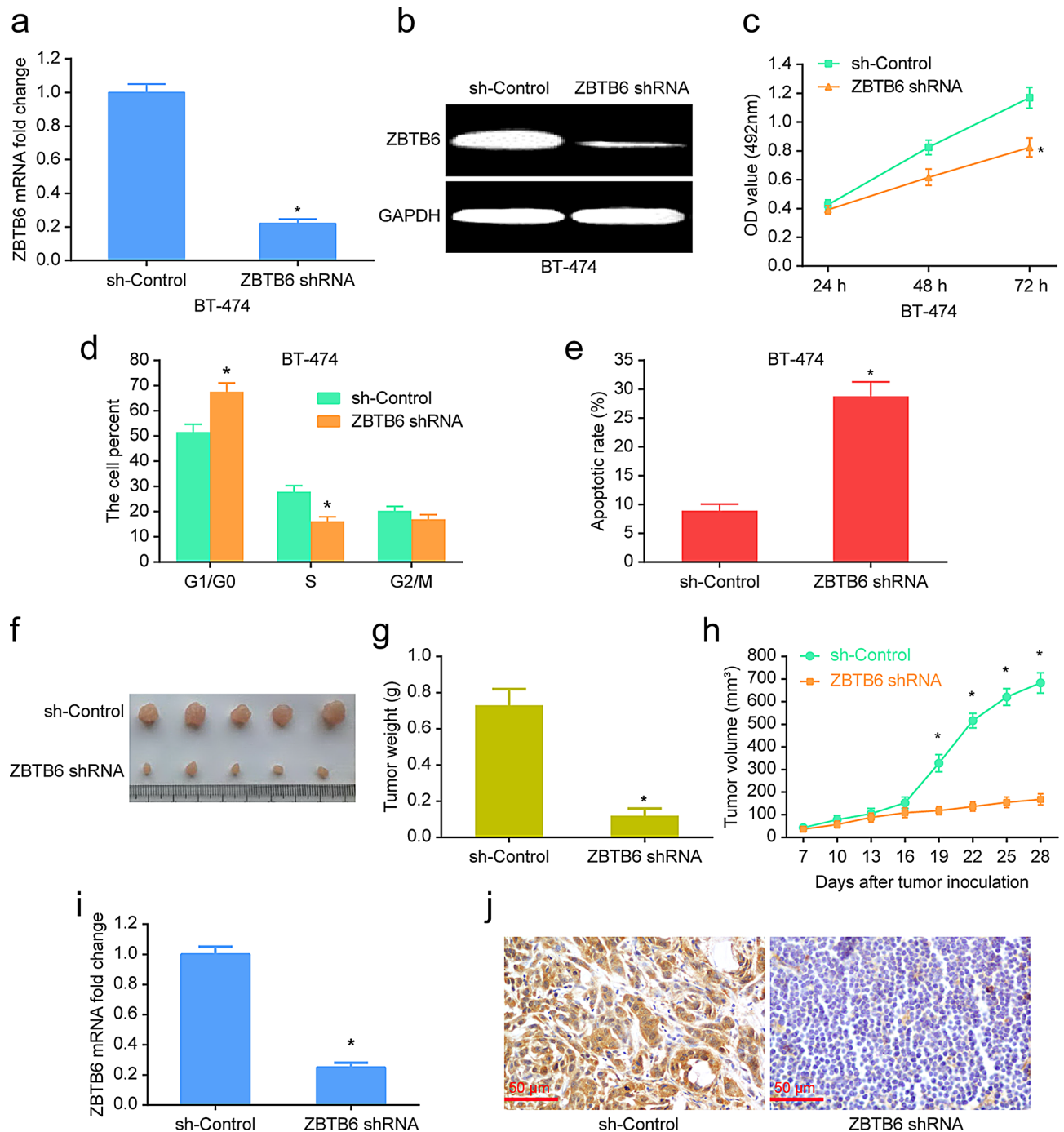


Fig. 3 ZBTB6 shRNA inhibits BC cell proliferation and promotes apoptosis in vitro and in vivo. **(a)** ZBTB6 mRNA expression after ZBTB6 knockdown in BC cells. GAPDH was used as an internal reference. **(b)** ZBTB6 protein expression after ZBTB6 knockdown in BC cells. GAPDH was used as an internal reference. **(c)** Viability of BC cells after ZBTB6 knockdown. **(d)** The cell cycle distribution of BC cells after ZBTB6 knockdown was analyzed via flow cytometry. **(e)** Apoptosis of BC cells after ZBTB6 knockdown was analyzed via flow cytometry. **(f)** Morphology of isolated tumors from nude mice. **(g)** Tumor weights of the indicated mice on the 31st day. **(h)** Growth curves of tumor volume were obtained from 7 to 31 days. **(i)** ZBTB6 mRNA expression in xenograft tumors. GAPDH was used as an internal reference. **(j)** Immunohistochemical staining was performed to detect the expression of ZBTB6. Each experiment was performed in triplicate. The quantitative data in **(c, h)** were analyzed via Pearson's chi-square test, and the quantitative data in **(a, d, e, g, h, and i)** were analyzed via Student's t test, * $p < 0.05$

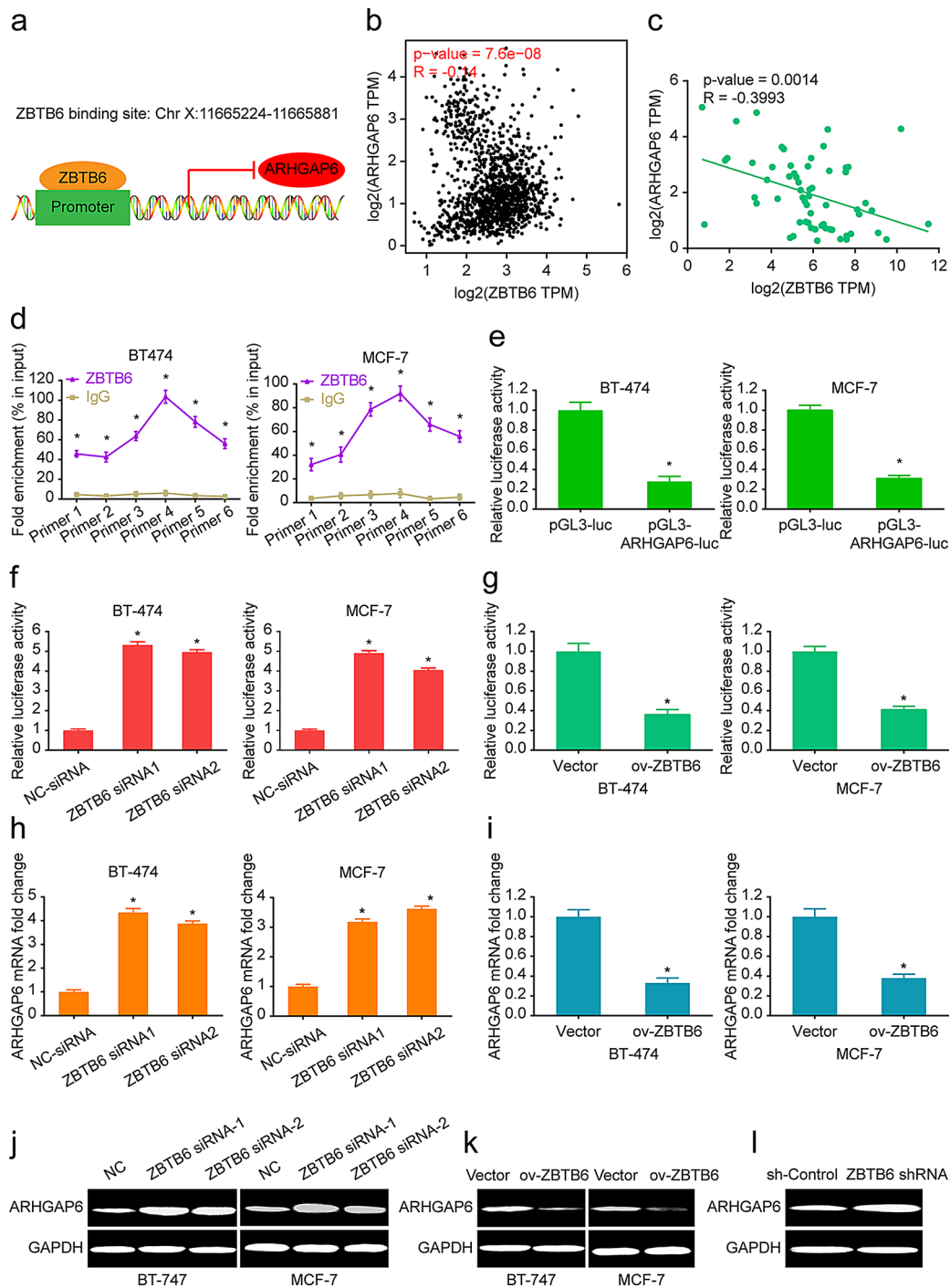


Fig. 4 ZBTB6 binds the promoter of ARHGAP6 to mediate its transcription. **(a)** Bioinformatics analysis (Cistrome Data Browser) was used to predict the ZBTB6 binding site in the promoter of ARHGAP6. **(b)** Correlation analysis between ZBTB6 and ARHGAP6 using TCGA data. **(c)** mRNA correlation between ZBTB6 and ARHGAP6 in BC tissues. **(d)** ChIP-qRT-PCR analysis revealed that ZBTB6 binds the promoter of ARHGAP6. **(e)** BC cells were transfected with pGL3-ARHGAP6-luc (target sequences of ZBTB6), and the luciferase activity was examined at 48 h after transfection. Renilla luciferase was used as the internal control. **(f)** BC cells were cotransfected with pGL3-ARHGAP6-luc and ZBTB6 siRNAs, and the luciferase activity was determined. Renilla luciferase was used as the internal control. **(g)** BC cells were cotransfected with pGL3-ARHGAP6-luc and ZBTB6-overexpression plasmids, and the luciferase activity was determined. Renilla luciferase was used as the internal control. **(h)** ARHGAP6 mRNA expression after transfection with ZBTB6 siRNA in BC cells. GAPDH was used as an internal reference. **(i)** ARHGAP6 mRNA expression after transfection with the ZBTB6-overexpression plasmid in BC cells. GAPDH was used as an internal reference. **(j)** ARHGAP6 protein expression after transfection with ZBTB6 siRNA in BC cells. GAPDH was used as an internal reference. **(k)** ARHGAP6 protein expression after transfection with the ZBTB6-overexpression plasmid in BC cells. GAPDH was used as an internal reference. **(l)** ARHGAP6 protein expression after ZBTB6 knockdown in BC cells. GAPDH was used as an internal reference. Each experiment was performed in triplicate. The quantitative data in **(b, c, d)** were analyzed via two-way ANOVA, and the quantitative data in **(e-i)** were analyzed via Student's *t* test, * $p < 0.05$

increased ARHGAP6 expression in BT-747 and MCF-7 cells (Fig. 4h, j; $P < 0.01$), whereas the ZBTB6 overexpression vector significantly suppressed ARHGAP6 expression (Fig. 4i, k; $P < 0.01$). Additionally, consistent with the results obtained via ZBTB6 siRNAs, Western blotting confirmed the upregulation of ARHGAP6 in tumors derived from ZBTB6 shRNA-transduced BT-747 cells (Fig. 4l).

Low expression of ARHGAP6 occurs in BC and is associated with clinicopathologic features

Previous studies have identified ARHGAP6 as a potential prognostic marker in BC, with low ARHGAP6 expression correlated with decreased patient survival [18]. We further validated and expanded upon these findings through bioinformatics analysis. Data obtained from UALCAN indicated that ARHGAP6 expression was significantly downregulated in BC tissues compared with normal breast tissues (Fig. S1a, b; $P < 0.01$). Furthermore, the methylation level of ARHGAP6 was significantly increased, suggesting a tumor-suppressive role for ARHGAP6 (Fig. S1c; $P < 0.01$). Additionally, ARHGAP6 expression in BC tissues was found to be associated with individual cancer stage and TP53 mutation status (Fig. S1d, e; $P < 0.05$). qRT-PCR analysis of 61 BC tissues and matched adjacent nontumor tissues demonstrated that the mRNA expression of ARHGAP6 was markedly lower in BC tissues than in normal tissues (Fig. S1f; $P < 0.01$). Consistent with these findings, Western blotting revealed a significant decrease in ARHGAP6 protein expression in BC tissues (Fig. S1g).

ARHGAP6 inhibits BC cell proliferation and promotes apoptosis in vitro

ARHGAP6 plays a crucial role in regulating cell signaling pathways and influencing tumor growth. Previous studies have demonstrated that ARHGAP6 can inhibit BC growth by promoting ferroptosis [25]. To further elucidate the role of ARHGAP6 in BC, we independently transfected the ARHGAP6 overexpression vector and ARHGAP6 siRNAs into BT-747 and MCF-7 cells. Western blotting and qRT-PCR analyses revealed that the ARHGAP6 overexpression vector effectively increased ARHGAP6 expression in both BT-747 and MCF-7 cells, whereas ARHGAP6 siRNAs significantly decreased ARHGAP6 expression (Fig. 5a, b; $P < 0.01$). MTT assays revealed reduced viability of BC cells following ARHGAP6 overexpression (Fig. 5c; $P < 0.01$), whereas ARHGAP6 knockdown resulted in increased viability of BC cells (Fig. 5d; $P < 0.01$). Furthermore, flow cytometry analysis demonstrated that ARHGAP6 overexpression led to cell cycle arrest at the G0/G1 phase (Fig. 5e; $P < 0.01$) and an increased percentage of apoptotic cells (Fig. 5g; $P < 0.01$), whereas ARHGAP6 knockdown yielded the

opposite effects (Fig. 5f, h; $P < 0.01$). Notably, decreased ARHGAP6 has been reported in lung adenocarcinoma, leading to increased levels of p-STAT3 and downstream targets such as c-Myc and Survivin [19, 25, 26]. Consequently, we assessed the expression of genes related to cell proliferation and the apoptosis-related signaling pathways STAT3/Survivin and STAT3/c-Myc through Western blotting. Our results indicated that ARHGAP6 overexpression increased the protein expression levels of p-STAT3, survivin, and c-Myc in BC cells (Fig. 5b). In contrast, ARHGAP6 knockdown led to a decrease in the expression of these proteins (Fig. 5b). We further obtained consistent results by isolating nuclear proteins and detecting the level of p-STAT3 in the nucleus (Fig. S2a). Collectively, these findings suggest that ARHGAP6, as a transcriptional downstream target of ZBTB6, modulates the cell cycle and apoptosis by inhibiting the STAT3/Survivin and STAT3/c-Myc signaling pathways, thereby repressing BC progression.

ZBTB6 facilitates BC progression by modulating the STAT3 signaling pathway by inhibiting ARHGAP6 transcription

Next, we aimed to elucidate the oncogenic function of ZBTB6 through its regulation of ARHGAP6 transcription. The qRT-PCR and Western blotting results demonstrated that ZBTB6 overexpression led to downregulation of ARHGAP6 expression, whereas overexpressing ARHGAP6 offset the effects of ZBTB6 overexpression on ARHGAP6 expression (Fig. 6a, b; $P < 0.01$). MTT assays revealed that ARHGAP6 overexpression reversed the promoting effect of ZBTB6 overexpression on cell viability (Fig. 6c; $P < 0.01$). Additionally, flow cytometry analysis indicated that ARHGAP6 overexpression reversed the decrease in G0/G1 phase cells and the reduction in apoptosis, both of which were induced by ZBTB6 overexpression (Fig. 6d, e; $P < 0.01$).

Moreover, we investigated key molecules within the signaling pathway and found that ZBTB6 overexpression upregulated the protein expression of p-STAT3, survivin and c-Myc, accompanied by a downregulation of ARHGAP6 (Fig. 6b), which is consistent with ZBTB6 being a transcriptional upstream regulator of ARHGAP6. As anticipated, ARHGAP6 overexpression effectively reversed the increases in p-STAT3, survivin and c-Myc levels caused by ZBTB6 overexpression (Fig. 6b). We obtained consistent results by detecting nuclear p-STAT3 levels in cell lines as well as xenograft tumors, further illustrating the regulation of p-STAT3 by ZBTB6 (Fig. S2b, c). Collectively, these findings suggest that ZBTB6 activates the STAT3 signaling pathway and subsequent cell survival signaling pathways by inhibiting ARHGAP6 transcription, thereby facilitating BC progression.

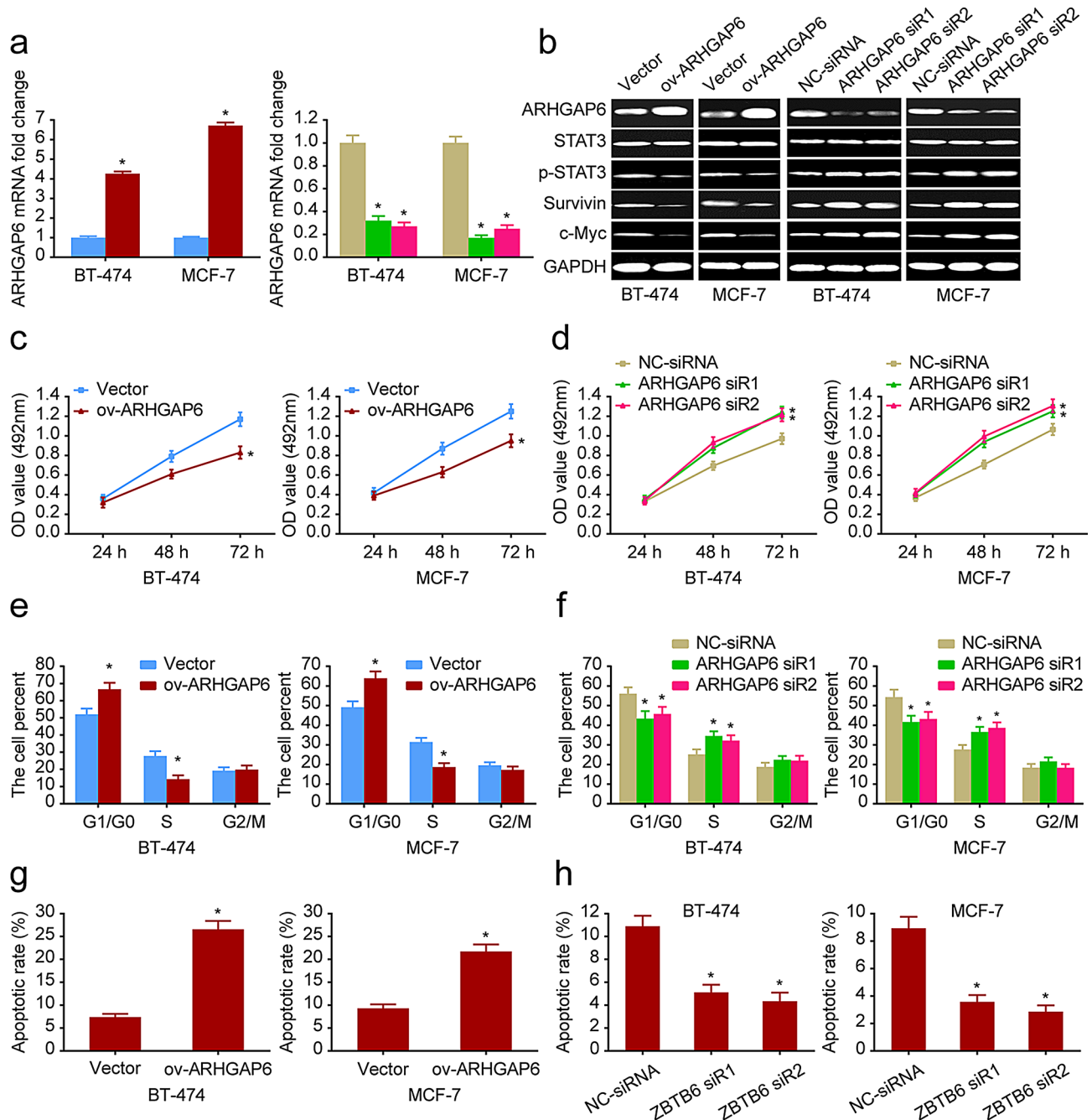


Fig. 5 ARHGAP6 inhibits BC cell proliferation and promotes apoptosis in vitro. **(a)** ARHGAP6 mRNA expression after transfection with ARHGAP6 siRNA and the ARHGAP6-overexpression plasmid in BC cells. GAPDH was used as an internal reference. **(b)** ARHGAP6, STAT3, p-STAT3, Survivin and c-Myc expression was measured after BC cells were transfected with ARHGAP6 siRNA and the ARHGAP6-overexpression plasmid. GAPDH was used as an internal reference. **(c)** Viability of BC cells after transfection with ARHGAP6 siRNA. **(d)** Viability of BC cells after transfection with the ARHGAP6-overexpression plasmid. **(e)** The cell cycle of BC cells after transfection with ARHGAP6 siRNA was analyzed by flow cytometry. **(f)** The cell cycle of BC cells after transfection with the ARHGAP6-overexpression plasmid was analyzed by flow cytometry. **(g)** Apoptosis of BC cells after transfection with ARHGAP6 siRNA was examined via flow cytometry. **(h)** Apoptosis of BC cells after transfection with the ARHGAP6-overexpression plasmid was examined via flow cytometry. Each experiment was performed in triplicate. The quantitative data in **(a, e-h)** were analyzed via Student's t test, and the quantitative data in **(c, d)** were analyzed via Pearson's chi-square test; * $p < 0.05$

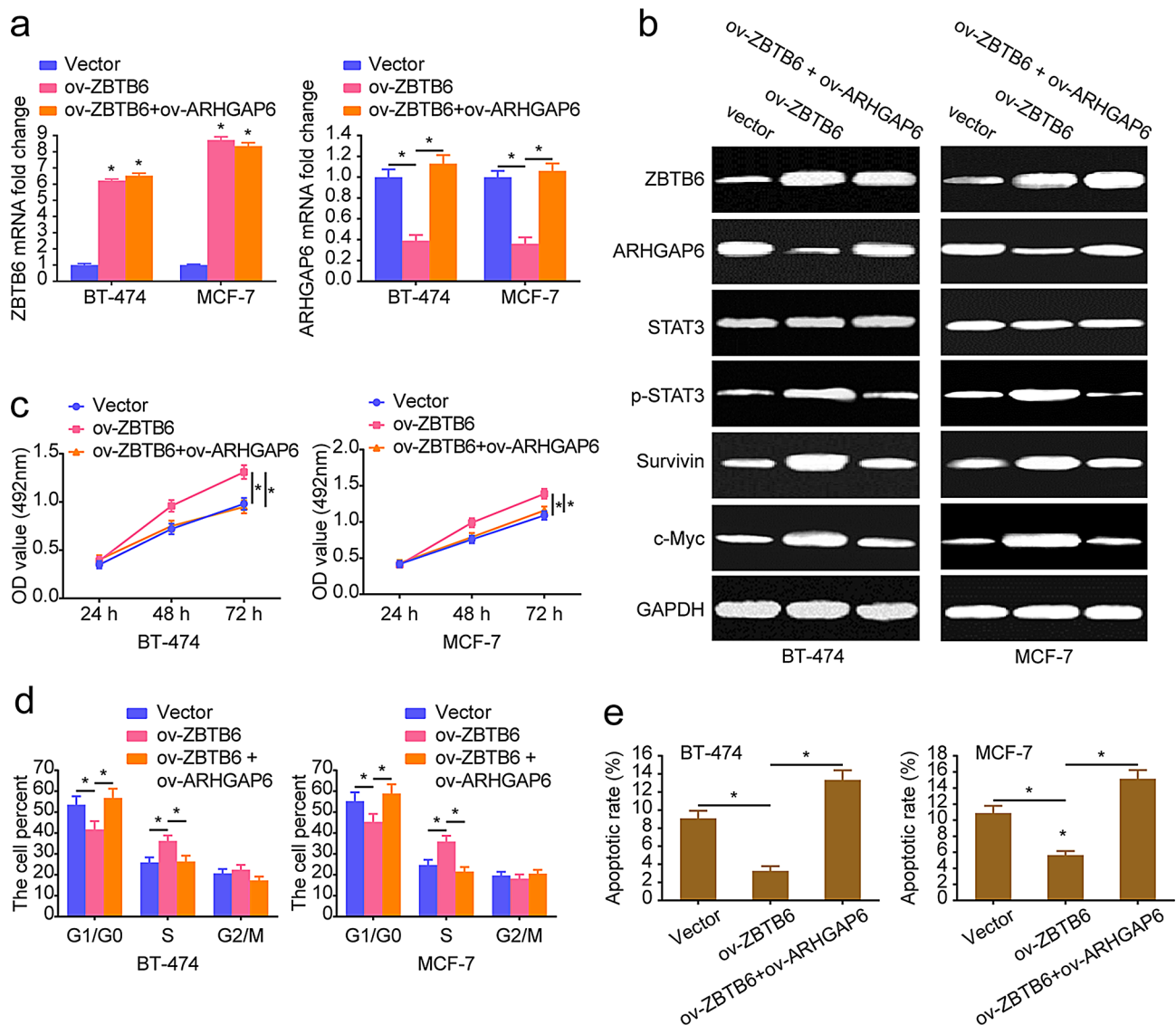


Fig. 6 ZBTB6 facilitates BC progression by modulating the STAT3 signaling pathway by inhibiting ARHGAP6 transcription. **(a)** ZBTB6 and ARHGAP6 mRNA expression after cotransfection with the ZBTB6-overexpression plasmid and ARHGAP6-overexpression plasmid. GAPDH was used as an internal reference. **(b)** ZBTB6, ARHGAP6, STAT3, p-STAT3, Survivin and c-Myc protein expression after cotransfection with the ZBTB6-overexpression plasmid and ARHGAP6-overexpression plasmid. GAPDH was used as an internal reference. Each experiment was performed in triplicate. **(c)** Viability of BC cells after cotransfection with the ZBTB6-overexpression plasmid and ARHGAP6-overexpression plasmid. **(d)** The cell cycle of BC cells after cotransfection with the ZBTB6-overexpression plasmid and ARHGAP6-overexpression plasmid was analyzed via flow cytometry. **(e)** Apoptosis of BC cells after cotransfection with the ZBTB6-overexpression plasmid and ARHGAP6-overexpression plasmid was analyzed via flow cytometry. The quantitative data in **(a, d, e)** were analyzed via Student's *t* test, and the quantitative data in **(c)** were analyzed via Pearson's chi-square test; **p* < 0.05

Discussion

With the use of mammography, magnetic resonance imaging (MRI), and various biomarkers, screening, diagnosis, and treatment of breast cancer have improved. However, as the most prevalent type of cancer among women and severely affects their quality of life and survival, breast cancer remains a major global public health challenge and is therefore a focus of biomedical research [27]. Researchers have aimed to deepen the understanding of breast cancer pathogenesis and molecular

characterization, thereby advancing the development of innovative therapeutic approaches. The onset and progression of breast cancer are closely linked to the dysregulation of multiple gene regulatory networks affecting transcription, posttranscriptional modifications and epigenetics. For example, mutations in key genes such as BRCA1 and BRCA2 are strongly associated with genetic susceptibility to breast cancer [28]. In addition, alterations in posttranscriptional regulatory mechanisms can lead to aberrant activation or inhibition of signaling

pathways, thereby promoting tumorigenesis [29]. Epigenetic studies are increasingly highlighting the importance of changes such as DNA methylation and histone modifications in processes such as the proliferation, migration and invasion of breast cancer cells. These changes not only determine the characteristics of the tumor but also may influence the response of the tumor to treatment [30]. While early detection and improved treatments can significantly improve survival rates, many patients are diagnosed at an advanced stage and therefore face a greater risk of death [31] (45). Breast cancer can be treated in a variety of ways, including surgical excision, chemotherapy, radiotherapy, targeted therapy and endocrine therapy. These treatments play different roles depending on the type and stage of the patient's cancer. However, despite the increasing number of treatment options available and technological advances, long-term survival remains suboptimal for many patients, especially if tumors recur despite multiple therapeutic interventions [32]. This situation suggests that current therapeutic strategies may not be sufficient to treat breast cancer comprehensively and effectively, highlighting the urgent need for the development of new biomarkers and chemotherapy targets.

The ZBTB is an evolutionarily conserved family of nuclear transcription factors [33] involved in cellular processes such as the DNA damage response, cell cycle progression, and a variety of developmental events, such as proto-gut embryo formation, organ formation, and hematopoietic stem cell fate determination [8, 33]. The role of the ZBTB family in hematopoietic cell development and tumor transformation has been extensively studied since the discovery of chromosomal translocations of ZBTB16 and BCL6 in acute promyelocytic leukemia and B-cell lymphoma in the 1990s [8, 33, 34]. The current literature primarily addresses hematological tumors: the promotion of cell cycle progression and malignant transformation of T cells by ZBTB17 through interaction with BCL6, GFI-1 and/or MYC [35]. ZBTB7A induces precursor T-cell lymphomas in mice by repressing the transcription of the tumor suppressor gene CDKN2a [36]. In addition, the roles of ZBTB proteins in solid tumors are under further investigation. Currently, ZBTB7A has been identified as a potential prognostic and immunoinfiltration biomarker to inhibit the progression of endometrial cancer [37]. BCL6 promotes glioma development and is an important therapeutic target [38]. ZBTB28 acts as a tumor suppressor in multiple types of carcinogenesis by targeting p53 in competition with BCL6 [39]. As an uncharacterized member of the ZBTB family, the biological effects and molecular mechanisms of ZBTB6 in cancer remain poorly understood. Despite the growing interest in other ZBTB family members, the specific role and significance of ZBTB6 in tumor biology

remain to be elucidated. Therefore, further investigations of the detailed biological functions of ZBTB6 and its related mechanisms in cancer development and progression are necessary. Our studies provide the first evidence that ZBTB6 is upregulated in both BC tissues and cell lines and that its expression is correlated with nodal metastasis, TP53 mutation status, and poor prognosis (Fig. 1). Through the knockdown and overexpression of ZBTB6 in BC cells, we subsequently demonstrated that ZBTB6 promotes cell viability, facilitates the cell cycle transition from the G0/G1 phase to the S phase, and inhibits apoptosis (Fig. 2). Non-p53-dependent apoptosis pathways, such as p21 activation [40], may further explain ZBTB6's role in BC cell survival. Correspondingly, cell-derived xenograft experiments revealed that ZBTB6 significantly enhances tumor growth in vivo (Fig. 3f-j). Collectively, these results indicate that ZBTB6 plays a crucial role in promoting BC cell growth and proliferation while inhibiting apoptosis, thereby contributing to the progression of breast cancer.

To further clarify the potential molecular mechanism by which ZBTB6 facilitates BC, we combined bioinformatics prediction, ChIP-qRT-PCR, and a dual-luciferase reporting system to determine whether ARHGAP6 is transcribed downstream of the ZBTB6 transcription factor (Fig. 4). ARHGAP6 has multiple key functions in cell biology, including regulating the cytoskeleton and influencing processes such as cell proliferation, migration and apoptosis. Moreover, the expression level of ARHGAP6 is closely associated with a variety of human diseases, especially cancer, where low expression of ARHGAP6 is significantly associated with tumorigenesis and progression, which may affect patient survival. In breast cancer, for example, downregulation of ARHGAP6 expression was associated with tumor progression, and its overexpression reduced cell proliferation and inhibited tumor growth by inducing a ferroptosis mechanism [25]. In this study, we verified that ARHGAP6 is downregulated in both BC tissues and cell lines and that its expression is correlated with individual cancer stage and TP53 mutation status (Fig. S1). On the other hand, our data demonstrated that ARHGAP6 could also decrease breast cancer cell viability, induce cell cycle arrest in the S phase and promote apoptosis, thereby inhibiting breast cancer progression (Fig. 5c-h).

ARHGAP6 has been reported to inhibit the intermediate RhoA, which directly activates STAT3 in the nucleus through tyrosine phosphorylation, and the activation of STAT3 is closely related to cell survival signaling pathways (such as survivin and c-Myc), thus influencing the cell cycle and apoptosis [19, 22–24, 42–44]. Given the effect of ARHGAP6 on the BC cell cycle and apoptosis, we speculate that ARHGAP6 could also regulate the STAT3/Survivin and STAT3/c-Myc signaling pathways

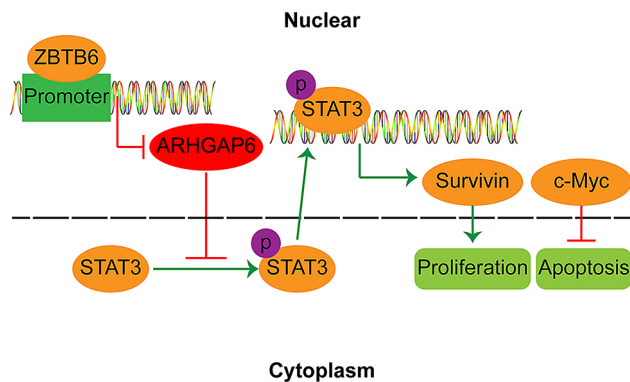


Fig. 7 Proposed model for the role of ZBTB6 in BC proliferation. ARHGAP6 could inhibit STAT3 activation and thus subsequent cell survival-related STAT3/Survivin and STAT3/c-Myc signaling pathways. In contrast, ZBTB6 can bind to the ARHGAP6 promoter and inhibit its transcription, thereby activating STAT3 and the subsequent STAT3/Survivin and STAT3/c-Myc signaling pathways, which in turn promotes breast cancer progression

in BC cells. As expected, the results showed that ARHGAP6 knockdown increased p-STAT3, survivin and c-Myc expression, whereas ARHGAP6 overexpression decreased the p-STAT3, survivin and c-Myc levels (Fig. 5a, b). Importantly, ZBTB6 overexpression upregulated p-STAT3, survivin and c-Myc expression (Fig. 6b). The reversed experiments for ZBTB6 overexpression via ARHGAP6 overexpression vectors subsequently revealed that ARHGAP6 overexpression reversed the promotion of cell viability and proliferation as well as the reduction in apoptosis caused by ZBTB6 overexpression (Fig. 6c-e). Furthermore, overexpressing ARHGAP6 reversed the increases in p-STAT3, survivin and c-Myc levels caused by ZBTB6 overexpression (Fig. 6b). These data illustrated that ZBTB6 could activate the STAT3 signaling pathway and subsequently cell survival signaling pathways by inhibiting ARHGAP6 transcription, thereby facilitating BC progression (Fig. 7).

This study elucidates the molecular mechanism by which ZBTB6 drives breast cancer progression through transcriptional repression of ARHGAP6 and subsequent activation of the STAT3 signaling pathway, while proposing clinically actionable strategies for translation. First, ZBTB6 expression levels may serve as a prognostic biomarker, enabling risk stratification and dynamic monitoring of therapeutic response via histopathological assays (such as immunohistochemistry) or liquid biopsies (such as circulating tumor DNA [ctDNA]) [45]. Second, targeting ZBTB6 with small-molecule inhibitors or gene-silencing technologies (such as siRNA/CRISPR) could block its oncogenic function, and combinatorial regimens with STAT3 inhibitors (such as Napabucasin) or chemotherapeutic agents may synergistically enhance efficacy and overcome drug resistance. Furthermore, restoring ARHGAP6 expression through epigenetic modulators (such as HDAC/DNMT inhibitors) or gene therapy

vectors could suppress the STAT3/Survivin/c-Myc axis, offering a novel approach to reverse tumor progression. In personalized oncology, ZBTB6 expression levels may guide therapeutic selection: patients with ZBTB6-high tumors may benefit preferentially from STAT3-targeted therapies or immune checkpoint inhibitor combinations (particularly in triple-negative breast cancer [TNBC]), whereas those with ZBTB6-low tumors might respond better to conventional chemotherapy. Future studies should focus on pharmacological optimization of ZBTB6 inhibitors, clinical trial design, and the role of ZBTB6 in metastasis and therapy resistance, thereby bridging mechanistic insights to clinical applications and advancing this target from bench to bedside [46].

Despite the promising implications of our findings, this study has several limitations that should be noted. First, the experimental findings are primarily based on established breast cancer cell lines (such as MCF-7, MDA-MB-231) and cell-derived xenograft (CDX) models, which may not fully recapitulate the heterogeneity of human tumors or the tumor microenvironment (TME), particularly stromal-immune interactions. This constraint could underestimate the functional diversity of ZBTB6 across breast cancer subtypes (such as HER2+) or metastatic contexts. Second, in vivo analyses relied on subcutaneous xenografts, which fail to model organ-specific metastatic niches (such as bone, lung) critical to clinical disease progression. Furthermore, while we identified ZBTB6 as a transcriptional repressor of ARHGAP6 leading to STAT3 activation, the structural domains of ZBTB6 responsible for this regulation (such as zinc finger motifs), its cooperative transcriptional partners, and posttranslational modifications (such as phosphorylation) remain uncharacterized, posing challenges for targeted drug development. Clinically, the biomarker potential of ZBTB6 requires validation in larger, multi-ethnic cohorts with diverse treatment histories. Additionally, the complexity of STAT3 signaling—including crosstalk with other oncogenic pathways (such as NF- κ B, PI3K/AKT)—may limit the efficacy of single-axis therapeutic strategies. These limitations could affect the generalizability of our conclusions, necessitating further validation through patient-derived organoids, genetically engineered mouse models (GEMMs), and multi-omics profiling to bridge mechanistic insights to clinical applications.

Conclusions

Overall, in this study, we are the first to reveal that ZBTB6 expression is upregulated in BC and promotes BC progression by modulating the STAT3 signaling pathway by inhibiting ARHGAP6 transcription (Fig. 7). This study suggests that ZBTB6 plays a crucial role in BC and

may be a promising prognostic indicator and potential chemotherapy target.

Abbreviations

BC	Breast cancer
ZBTB6	Specificity protein 4
qRT-PCR	Quantitative real-time PCR
BTB	Broad-complex, tram-track and bric-a-brac
ChIP	Chromatin immunoprecipitation
ARHGAP6	Rho GTPase-activating protein 6
GAPDH	Glyceraldehyde-3-phosphate dehydrogenase
PBS	Phosphate-buffered saline
UALCAN	University of Alabama at Birmingham Cancer Data Analysis Portal

Supplementary Information

The online version contains supplementary material available at <https://doi.org/10.1186/s12967-025-06364-y>.

Supplementary Material 1

Supplementary Material 2

Supplementary Material 3

Acknowledgements

Not applicable.

Author contributions

XT and CD designed the experiments; XT, CD, YL and SP conducted the experiments; NH and YZ provided materials and methods; XT, YL and SP analyzed the data; and CD wrote the manuscript. All authors read and approved the final manuscript.

Funding

This study was financially supported by the Natural Science Basic Research Program of Shaanxi (Program No. 2021JM-582) and the Xi'an Municipal Science and Technology Project (No. 2017113SF/YX007(4)).

Data availability

The datasets analyzed during the current study are available at <https://ualcan.path.uab.edu/> and <http://cistrome.org/db/#/>. All other data supporting the findings of this study are available in the manuscript, as well as from the corresponding authors upon reasonable request.

Declarations

Ethics approval and consent to participate

Ethical approval was given by the Ethics Committee of The First Affiliated Hospital of Xi'an Jiaotong University. The whole study was performed in accordance with the ethical standards of the 1964 Declaration of Helsinki and its later amendments.

Informed consent

Every individual patient who participated in the research signed written informed consent.

Consent for publication

The authors agreed to publish the research content in the manuscript.

Competing interests

The authors declare that they have no competing interests.

Received: 16 November 2024 / Accepted: 8 March 2025

Published online: 25 March 2025

References

- Greenlee H, DuPont-Reyes MJ, Balneaves LG, Carlson LE, Cohen MR, Deng G, et al. Clinical practice guidelines on the evidence-based use of integrative therapies during and after breast cancer treatment. *CA Cancer J Clin*. 2017;67:194–232.
- Sung H, Ferlay J, Siegel RL, Laversanne M, Soerjomataram I, Jemal A, et al. Global cancer statistics 2020: GLOBOCAN estimates of incidence and mortality worldwide for 36 cancers in 185 countries. *CA Cancer J Clin*. 2021;71:209–49.
- Effects of chemotherapy. And hormonal therapy for early breast cancer on recurrence and 15-year survival: an overview of the randomized trials. *Lancet*. 2005;365:1687–717.
- Gradishar WJ, Moran MS, Abraham J, Aft R, Agnese D, Allison KH, et al. NCCN Guidelines(R) insights: breast cancer, version 4.2021. *J Natl Compr Canc Netw*. 2021;19:484–93.
- Akram M, Iqbal M, Daniyal M, Khan AU. Awareness and current knowledge of breast cancer. *Biol Res*. 2017;50:33.
- Wilkinson L, Gathani T. Understanding breast cancer as a global health concern. *Br J Radiol*. 2022;95:20211033.
- Lee SU, Maeda T. POK/ZBTB proteins: an emerging family of proteins that regulate lymphoid development and function. *Immunol Rev*. 2012;247:107–19.
- Maeda T. Regulation of hematopoietic development by ZBTB transcription factors. *Int J Hematol*. 2016;104:310–23.
- Piazza F, Costoya JA, Merghoub T, Hobbs RM, Pandolfi PP. Disruption of PLZF in mice leads to increased T-lymphocyte proliferation, cytokine production, and altered hematopoietic stem cell homeostasis. *Mol Cell Biol*. 2004;24:10456–69.
- Daniel JM. Dancing in and out of the nucleus: p120(ctn) and the transcription factor Kaiso. *Biochim Biophys Acta*. 2007;1773:59–68.
- Parekh S, Prive G, Melnick A. Therapeutic targeting of the BCL6 oncogene for diffuse large B-cell lymphomas. *Leuk Lymphoma*. 2008;49:874–82.
- Polo JM, Dell'Oso T, Ranuncolo SM, Cerchiotti L, Beck D, Da Silva GF, et al. Specific peptide interference reveals BCL6 transcriptional and oncogenic mechanisms in B-cell lymphoma cells. *Nat Med*. 2004;10:1329–35.
- Cao X, Lu Y, Zhang X, Kovalovsky D. Zbtb1 safeguards genome integrity and prevents p53-Mediated apoptosis in proliferating lymphoid progenitors. *J Immunol*. 2016;197:1199–211.
- Zhu C, Chen G, Zhao Y, Gao XM, Wang J. Regulation of the development and function of B cells by ZBTB transcription factors. *Front Immunol*. 2018;9:580.
- Zheng W, Chen C, Yu J, Jin C, Han T. An energy metabolism-based eight-gene signature correlates with the clinical outcome of esophagus carcinoma. *BMC Cancer*. 2021;21:345.
- Chunyu Huang P, Lin J, Wang. Zhongxi Huang. [Differential gene expression profiling for identification of protective transcription factors in different subtypes of nasopharyngeal carcinoma]. *Nan Fang Yi Ke Da Xue Xue Bao*. 2013;33:1565–70.
- Wu Y, Xu M, He R, Xu K, Ma Y. ARHGAP6 regulates the proliferation, migration and invasion of lung cancer cells. *Oncol Rep*. 2019;41:2281–888.
- Chen WX, Lou M, Cheng L, Qian Q, Xu LY, Sun L, et al. Bioinformatics analysis of potential therapeutic targets among ARHGAP genes in breast cancer. *Oncol Lett*. 2019;18:6017–25.
- Li P, Lv H, Xu M, Zang B, Ma Y. ARHGAP6 promotes apoptosis and inhibits Glycolysis in lung adenocarcinoma through STAT3 signaling pathway. *Cancer Manag Res*. 2020;12:9665–78.
- Li J, Liu Y, Yin Y. Inhibitory effects of Arhgap6 on cervical carcinoma cells. *Tumor Biol*. 2016;37:1411–25.
- Chen W, Tan M, Yu C, Liao G, Kong D, Bai J, et al. ARHGAP6 inhibits bladder cancer cell viability, migration, and invasion via beta-catenin signaling and enhances mitomycin C sensitivity. *Hum Cell*. 2023;36:786–97.
- Aznar S, Valeron PF, Del RS, Perez LF, Perona R, Lacal JC. Simultaneous tyrosine and Serine phosphorylation of STAT3 transcription factor is involved in Rho A GTPase oncogenic transformation. *Mol Biol Cell*. 2001;12:3282–94.
- Prakash SK, Paylor R, Jenna S, Lamarche-Vane N, Armstrong DL, Xu B. Functional analysis of ARHGAP6, a novel GTPase-activating protein for RhoA. *Hum Mol Genet*. 2000;9:477–88.
- Schaefer L, Prakash S, Zoghbi HY. Cloning and characterization of a novel rho-type GTPase-activating protein-encoding gene (ARHGAP6) from the critical region for microphthalmia with linear skin defects. *Genomics*. 1997;46:268–77.
- Fu L, Jin Q, Dong Q, Li Q. AATF is overexpressed in human head and neck squamous cell carcinoma and regulates STAT3/Survivin signaling. *Oncotargets Ther*. 2021;14:5237–48.

26. Amaya ML, Inguva A, Pei S, Jones C, Krug A, Ye H, et al. The STAT3-MYC axis promotes survival of leukemia stem cells by regulating SLC1A5 and oxidative phosphorylation. *Blood*. 2022;139:584–96.
27. Bray F, Ferlay J, Soerjomataram I, Siegel RL, Torre LA, Jemal A. Global cancer statistics 2018: GLOBOCAN estimates of incidence and mortality worldwide for 36 cancers in 185 countries. *CA Cancer J Clin*. 2018;68:394–424.
28. Miki Y, Swensen J, Shattuck-Eidens D, Futreal PA, Harshman K, Tavtigian S, et al. A strong candidate for the breast and ovarian cancer susceptibility gene BRCA1. *Science*. 1994;266:66–71.
29. Anastasiadou E, Jacob LS, Slack FJ. Noncoding RNA networks in cancer. *Nat Rev Cancer*. 2018;18:5–18.
30. Kouzarides T. Chromatin modifications and their function. *Cell*. 2007;128:693–705.
31. Siegel RL, Miller KD, Fuchs HE, Jemal A, Cancer, Statistics. 2021. *CA Cancer J Clin*. 2021;71:7–33.
32. Cardoso F, Kyriakides S, Ohno S, Penault-Llorca F, Poortmans P, Rubio IT, et al. Early breast cancer: ESMO clinical practice guidelines for diagnosis, treatment and follow-up. *Ann Oncol*. 2019;30:1194–220.
33. Kelly KF, Daniel JM. POZ for effect—POZ-ZF transcription factors in cancer and development. *Trends Cell Biol*. 2006;16:578–87.
34. Siggs OM, Beutler B. The BTB-ZF transcription factors. *Cell Cycle*. 2012;11:3358–69.
35. Ross J, Rashkovan M, Fraszczak J, Joly Beuparlant C, Vadnais C, Winkler R, et al. Deletion of the Miz-1 POZ domain increases efficacy of cytarabine treatment in T- and B-ALL/Lymphoma mouse models. *Cancer Res*. 2019;79:4184–95.
36. Maeda T, Hobbs RM, Merghoub T, Guenah I, Zelent A, Cordon-Cardo C, et al. Role of the proto-oncogene *Pokemon* in cellular transformation and ARF repression. *Nature*. 2005;433:278–85.
37. Geng R, Zheng Y, Zhou D, Li Q, Li R, Guo X. ZBTB7A, a potential biomarker for prognosis and immune infiltrates, inhibits progression of endometrial cancer based on bioinformatics analysis and experiments. *Cancer Cell Int*. 2020;20:542.
38. Xu L, Chen Y, Dutra-Clarke M, Mayakonda A, Hazawa M, Savinoff SE, et al. BCL6 promotes glioma and serves as a therapeutic target. *Proc Natl Acad Sci USA*. 2017;114:E4317.
39. Xiang T, Tang J, Li L, Peng W, Du Z, Wang X, et al. Tumor suppressive BTB/POZ zinc-finger protein ZBTB28 inhibits oncogenic BCL6/ZBTB27 signaling to maintain p53 transcription in multiple carcinogenesis. *Theranostics*. 2019;9:8182–95.
40. Rajabi L, Ebrahimdoost M, Mohammadi SA, et al. Aqueous and ethanolic extracts of *Moringa Oleifera* leaves induce selective cytotoxicity in Raji and Jurkat cell lines by activating the P21 pathway independent of P53. *Mol Biol Rep*. 2025;52:102. <https://doi.org/10.1007/s11033-024-10200-9>.
41. Chen X, Zhu J, Li X, Chen J, Zhou Z, Fan X, et al. ARHGAP6 suppresses breast cancer tumor growth by promoting ferroptosis via RhoA-ROCK1-p38 MAPK signaling. *Front Biosci (Landmark Ed)*. 2024;29:6.
42. Wei YH, Liao SL, Wang SH, Wang CC, Yang CH. Simvastatin and ROCK inhibitor Y-27632 inhibit myofibroblast differentiation of graves' Ophthalmopathy-Derived orbital fibroblasts via RhoA-Mediated ERK and p38 signaling pathways. *Front Endocrinol (Lausanne)*. 2020;11:607968.
43. Zhou H, Sun Y, Zhang L, Kang W, Li N, Li Y. The RhoA/ROCK pathway mediates high glucose-induced cardiomyocyte apoptosis via oxidative stress, JNK, and p38MAPK pathways. *Diabetes Metab Res Rev*. 2018;34:e3022.
44. Shen Y, Zhang Y, Du J, Jiang B, Shan T, Li H, et al. CXCR5 downregulation alleviates cognitive dysfunction in a mouse model of sepsis-associated encephalopathy: potential role of microglial autophagy and the p38MAPK/NF-kappaB/STAT3 signaling pathway. *J Neuroinflammation*. 2021;18:246.
45. Aghaei M, Khademi R, Bahreiny SS, Saki N. The need to Establish and recognize the field of clinical laboratory science (CLS) as an essential field in advancing clinical goals. *Health Sci Rep*. 2024;7(8):e70008.
46. Saki N, Haybar H, Aghaei M, Subject. Motivation can be suppressed, but scientific ability cannot and should not be ignored. *J Translational Med*. 2023;21(1):520.

Publisher's note

Springer Nature remains neutral with regard to jurisdictional claims in published maps and institutional affiliations.